Groundwater age investigation of eskers in the Amos region, Quebec, Canada

Christine Boucher [a], Daniele L. Pinti [a,d,*], Martin Roy [a], M. Clara Castro [b], Vincent Cloutier [c], Daniel Blanchette [c], Marie Larocque [a], Chris M. Hall [b], Tao Wen [b], Yuji Sano [d]

[a] GEOTOP and Département des sciences de la Terre et de l'atmosphère, Université du Québec à Montréal, CP8888 succ. Centre-Ville, Montréal, QC, Canada
[b] Department of Earth and Environmental Sciences, University of Michigan, 1100 N. University, Ann Arbor, MI 48109-1005, USA
[c] Groupe de recherche sur l'eau souterraine, Institut de recherche en mines et en environnement, Université du Québec en Abitibi-Témiscamingue, Campus d'Amos, Amos, QC, Canada
[d] Atmosphere and Ocean Research Institute, The University of Tokyo, Kashiwa, Chiba 277-8564, Japan

ARTICLE INFO

SUMMARY

Noble gases, in particular $^3He/^4He$ (R) ratios, were measured together with tritium activity in groundwater from eskers and moraines of the Abitibi-Temiscamingue region of northwestern Quebec (eastern Canada). These high-latitude glaciofluvial landforms contain precious freshwater resources that need to be quantified. Here we provide estimates of residence time for groundwater in glaciofluvial sediments forming the Saint-Mathieu–Berry (SMB) and Barraute eskers, the Harricana moraine and in the underlying fractured bedrock aquifer. The $^3He/^4He$ ratios range from 0.224 ± 0.012 to 1.849 ± 0.036Ra, where Ra is the atmospheric $^3He/^4He$ ratio (1.386×10^{-6}). These results suggest the occurrence of ^3He produced by decay of tritium and terrigenic ^4He produced by decay of U and Th. Calculated $^3H/^3He$ apparent ages of groundwater from the SMB esker and the Harricana moraine range from 6.6 ± 1.1 a to 32 ± 7.4 a. Terrigenic ^4He ($^4He_{terr}$) was found in the deeper wells of the SMB esker and in the wells tapping water from the deeper fractured aquifer located below the eskers and moraines and confined by postglacial clays. The amount of $^4He_{terr}$ ranges from 3.4×10^{-9} to 2.2×10^{-6} cm^{3}STP g^{-1} and shows a clear gradient with depth, suggesting addition of a $^4He_{terr}$ flux entering the bottom of the eskers. Modeled $^4He_{terr}$ fluxes range from 2.0×10^{-8} cm^{3}STP cm^{-2} yr^{-1} at the Harricana moraine to 6.6×10^{-7} cm^{3}STP cm^{-2} yr^{-1} in the southern section of the SMB esker. Calculated fluxes are highly variable and 5–165 times lower than the helium continental crustal flux, suggesting local helium sources, with helium being driven upward through preferential pathways such as local faults. Maximum $U–Th/^4He$ ages obtained for the groundwater in the fractured bedrock range from 1473 ± 300 a to 137 ± 28 ka, suggesting the occurrence of several generations of fossil meltwater trapped under the clay plain after the last two glaciations.

© 2015 Elsevier B.V. All rights reserved.

1. Introduction

Continental areas of the Northern Hemisphere, notably Canada, were severely affected by ice cover during the late Pliocene and Pleistocene. A wide range of glacial and deglacial landforms were formed during this period, notably eskers, which consist in long, linear and relatively narrow ridges composed of stratified sand and gravel. Eskers were mainly deposited within ice-walled tunnels by highly organized meltwater flow systems (e.g., Banerjee and McDonald, 1975; Shilts et al., 1987; Clark and Walder, 1994). Moraines also represent heterogeneous accumulations of sand and gravel that were generally deposited at or near the ice margin during ice retreat. From a hydrogeological perspective, these landforms (eskers and moraines) may be considered equivalent entities due to their similar composition (sorted granular material).

The last deglaciation in the Abitibi-Temiscamingue region, Quebec (Fig. 1), was marked by the breakup of the ice margin into two lobes, as recorded by the Harricana interlobate moraine, a large body of sand and gravel oriented north–south that extends for several hundred kilometers (Veillette, 1996; Dyke, 2004). Ice retreat resulted in the deposition of eskers that show two different trends: those oriented NW–SE to the west of the Harricana moraine, and those oriented NE–SW to the east of this major landform (Veillette et al., 2004, 2007). Meltwater produced during the deglaciation also led to the development of Lake Ojibway, a large proglacial lake that inundated the area. As a result, thick accumulations of fine-grained

rhythmites (clay and silt) cover entirely or partially most eskers, thereby forming confined or semi-confined aquifers, with porosity reaching up to 30% near the core of the landform. The groundwater has generally very low salinity and excellent organoleptic characteristics as drinking water, which is commercialized as the bottled water ESKA® near the city of Amos. Accordingly, these eskers and the Harricana moraine represent an important water resource in this area, as its quality is superior to slightly salty groundwater from the fractured bedrock. The hydraulic regime of these systems is not fully understood, mainly because of the spatial complexity and heterogeneous character of these glaciofluvial deposits (Boulton et al., 1995, 2009).

The hydrogeology of this area has been recently the focus of a study by the *Université du Québec en Abitibi-Témiscamingue* (UQAT) (Cloutier et al., 2011, 2013). The goals of this study were to better understand the hydraulic regime of eskers and moraines, and to assess their potential as a long-term source of drinking water in the region, as well as to evaluate their vulnerability to pollution (Cloutier et al., 2013). Except for a few unpublished ^{14}C ages (Riverin, 2006) and ^{3}H measurements (Castelli, 2012), there are no chronological constraints on the groundwater of this region. The aim of this work was to fill this gap by producing ^{3}H/[3]He and U–Th/[4]He residence times based on noble gases measurements of groundwater, and to provide a basis for future high-resolution groundwater age surveys.

2. Geology and hydrogeology of the studied area

The study area (Fig. 1a) has a surface area of 860 km^2 and includes the municipalities of Amos, Barraute, La Motte and Landrienne, in Abitibi-Temiscamingue, Quebec, Canada. This region lies on crystalline bedrock of the Canadian Shield, more specifically in the Abitibi greenstone belt of the Superior Province, which is upper Archean in age (2.85–2.65 Ga). The bedrock is composed of mafic to intermediate volcanic rocks intercepted by lenses of felsic volcanic rocks and metasediment belts (wacke, conglomerates and iron formations). These lithologies are intruded by Archean granitic and tonalitic plutons (and later by Proterozoic diabases) and crosscut by gneissic rocks (Weber and Latulippe, 1964). Precambrian metamorphic rocks constitute an aquifer characterized by a low hydraulic conductivity whose potential increases locally with fractures and fissures (Cloutier et al., 2007).

The Abitibi-Temiscamingue region was completely covered by the Laurentide Ice Sheet during the last glacial cycle and deglaciation began at ~9 ka (Dyke, 2004). Progressive thinning of the ice margin led to the isolation of the Hudson Bay ice dome and the New-Quebec ice dome, in between which a major complex of glaciofluvial sediments was deposited (the Harricana interlobate moraine; Fig. 1) along with a dense network of eskers (Veillette et al., 2003). Subsequent ice retreat occurred away from the Harricana glaciofluvial sediment complex, toward the northwest and northeast, in contact with the waters of glacial Lake Ojibway (Veillette, 1994; Roy et al., 2011). These deglacial landforms are composed of heterometric and chaotic accumulations of pebble, gravel and sand derived from the glacial erosion of the local Archean bedrock (Veillette et al., 2004). The study area is crossed, from west to east, by three major glaciofluvial bodies: the Saint-Mathieu–Berry (hereafter denoted as SMB) esker, the Harricana interlobate moraine and the Barraute esker (Fig. 1a). The SMB esker is 120 km in length, 25–45 m thick, and 1–5 km wide. The Harricana moraine is the most voluminous in the region, with a total length of 278 km and a maximum width of 4.4 km. The Barraute esker is 20 km in length, with height and width resembling the SMB esker.

Eskers and moraine are deposited on the Precambrian bedrock, sometimes separated by glacial deposits (tills). Glacial deposits can be continuous with a thickness of several meters or discontinuous with a thickness of less than 1 meter (Cloutier et al., 2013). Often isolated patches of tills are found in glacially scoured bedrock depressions, protected from glacial erosion. The extension of these deposits under the eskers is difficult to evaluate because they are often mixed with glaciofluvial deposits (Cloutier et al., 2013).

The presence of Lake Ojibway left a strong imprint on the landscape (Roy et al., 2011). Thick accumulations of fine-grained glaciolacustrine sediments cover most deglacial features (eskers and ice-marginal deposits, such as moraines). The vast expanses of Ojibway clay form a very low permeability unit, which might confine totally or partially the esker's aquifers (Veillette et al., 2004). The Ojibway clay plain is broken in places by rare bedrock knobs (hills) and the crests of some eskers or the Harricana moraine (Fig. 1a). Eskers deposited near the former lake level may be reworked into beaches onto their crests or flanks, whereas eskers deposited in deep-water conditions may be associated with subaqueous outwash fans.

This particular depositional environment led to a classification of eskers of the Abitibi-Temiscamingue region into four types (A–D) on the basis of the depositional setting and sedimentological characteristics of the confined and unconfined eskers (Veillette et al., 2004, 2007; Nadeau, 2011). In the study area, eskers are of type C, which consists in eskers and moraines partially confined by clay (SMB and Harricana), and of type D that consists in eskers completely buried by clay (parts of SMB and Barraute). This classification may vary for a given esker, mainly due to changes in the clay cover along its length. Direct recharge from precipitation occurs in partially confined aquifers (eskers type C) while recharge areas of buried landforms (such as Barraute esker) remain to be fully determined. For example, the Harricana moraine, located about 10 km to the west of the buried Barraute esker, could correspond to its recharge zone (Veillette et al., 2007). This moraine, partially covered by clays and characterized by a high permeability, is directly recharged by rainfall. Accordingly, water from this formation is expected to be young. South of this moraine, the elevated zone of Mont Video (Fig. 1a) could be a preferential recharge zone for both the Harricana moraine and the nearby Barraute esker (buried). In the SMB esker, two types of flow were documented (Riverin, 2006). One is longitudinal and controlled by the topography of bedrock, with water moving from the southern and northern elevated zones toward the center of the esker. The second flow is transversal to the esker and originates from infiltration toward the edge of the esker and is subsequently diffused into bogs or contact zones between clay and gravel.

Groundwater flows rapidly within the highly porous (porosity ~25–30%) and permeable gravel aquifers formed by eskers. A detailed geochemical study of springs associated with eskers showed that the water is mainly of Ca–HCO$_3$ type, with average total dissolved solids (TDS) of 87 mg L^{-1} (Castelli et al., 2011). However, the bedrock is locally fractured and local aquifers show higher salinities reaching 760 mg L^{-1} (Table 1). Riverin (2006) estimated qualitatively groundwater residence times for the SMB esker. Tritium (^{3}H) measurements and uncorrected ^{14}C ages pointed to the presence of an active (top part of the aquifer) and a less active (lower portions of the confined aquifer) flow zones. Based on uncorrected ^{14}C ages, these zones might contain modern (1–25 a), intermediate (300–6000 a) and fossil groundwater (>6000 a) (Riverin, 2006).

3. Sampling and analytical methods

A total of fifteen groundwater samples (Fig. 1a; Tables 1 and 3) were collected in the study area during the summers of 2011
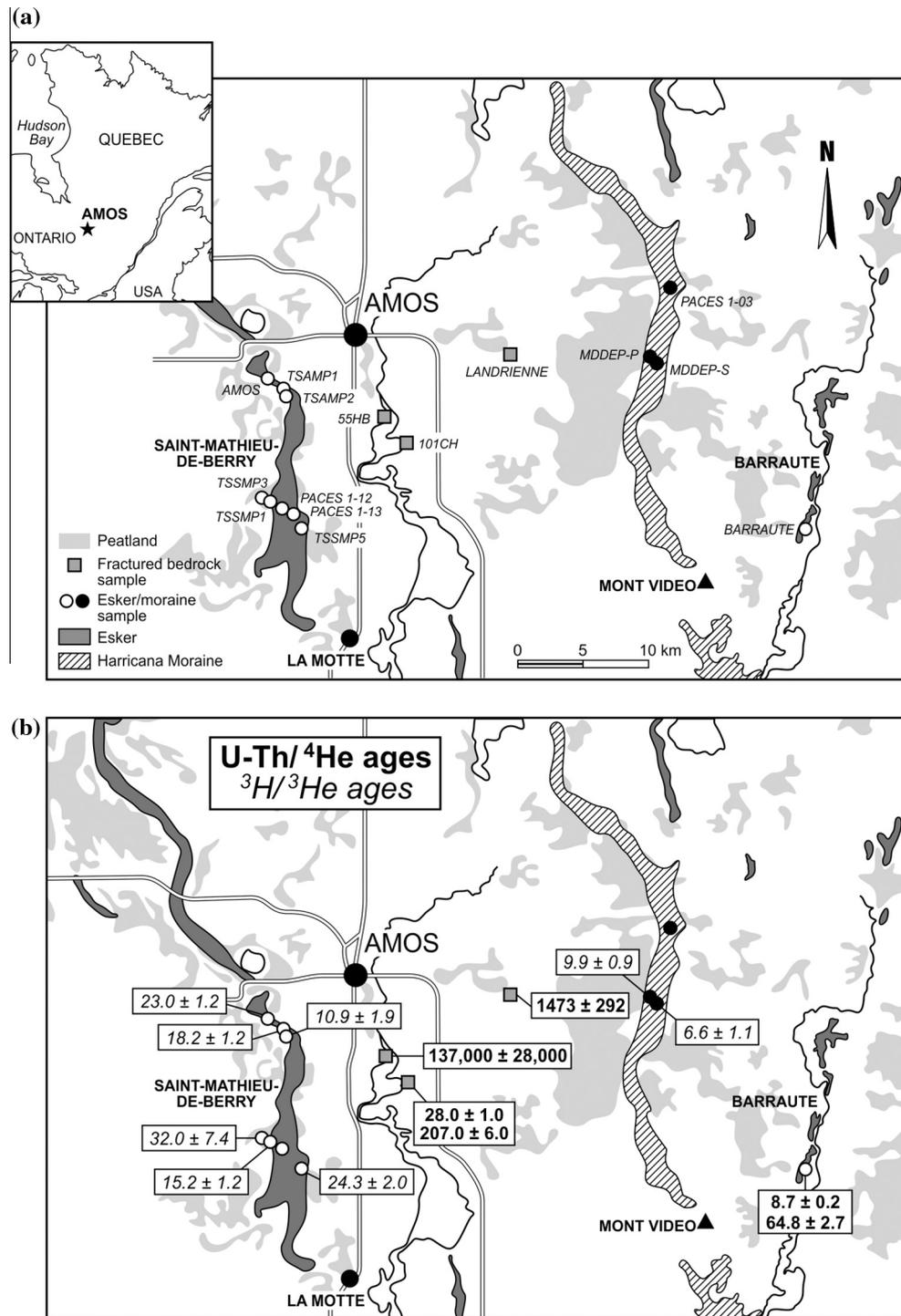
Fig. 1. (a) Schematic geographical map of the study area with the localization of samples in Saint-Mathieu–Berry and Barraute eskers (white dots), in the Harricana interlobate moraine (black dots) and from the fractured rock aquifer under the clay plain (gray squares); (b) with $^3H/^3He$ groundwater apparent ages and U–Th/^4He ages (in bold).

(12 samples) and 2012 (3 samples). In the fractured bedrock aquifer underlying the clay plain, one sample was collected from the municipality well of Landrienne and two others located in the same aquifer were collected from domestic wells (101CH and 55HB; Fig. 1a). Two wells drilled by the Ministry of Environment of the Province of Quebec (MDDEP-S and MDDEP-P) and one well drilled by UQAT (PACES 1-03) were sampled from the Harricana moraine. The municipal well of Barraute was sampled from the Barraute esker. The Amos municipal well and seven wells drilled and instrumented by UQAT were sampled from the SMB esker

(TSAM-P1, P2, TSSM-P1, P3, P5, PACES 1-12, 1-13). One of them, TSSMP-3, is a flowing artesian well.

Wells in the fractured bedrock (Landrienne, 55HB and 101CH) have no casing. All other MDDEP and UQAT drilled wells have a casing and short screens of 1.5 m long, except for well TSSM-P5 (3 m) and Barraute (4.6 m; Table 2). Amos municipality is a multidrain well (Feldman-type), consisting of 8 horizontal drains departing from the base of the vertical borehole with lengths variable between 7.2 and 45.8 m and a diameter of 0.2 m. Screens cover between 70% and 90% of the drain's length.

Table 1
Noble gas concentrations and He, Ne and Ar isotopic ratios in groundwater of Amos region, Abitibi-Temiscamingue.

Well name	Coordinates	Coordinates	Altitude	Well depth	TDS	T	pH	^{4}He	^{20}Ne	^{36}Ar	^{84}Kr	^{132}Xe	$(^3$He/^{4}He$)_{meas}$	^{20}Ne/^{22}Ne	^{21}Ne/^{22}Ne	^{38}Ar/^{36}Ar	^{40}Ar/^{36}Ar
	Longitude UTM NAD 83 Z17	Latitude	(m)	(m)	(mg L^{-1})	(°C)			cm^{3}STP g^{-1} × 10^{-7}				$(^3$He/^{4}He$)_{AIR}$ R/Ra				
Saint-Mathieu–Berry esker																	
Amos municipality	706095	5379631	312.3	23.34	106	9.4	8.3	0.59	1.83	13.56	0.521	0.0362	1.849 ± 0.036	9.91 ± 0.03	0.0278 ± 0.0002	0.1880 ± 0.0010	294.4 ± 1.0
PACES 1-12	707125	5370880	337.9	53.51	103	5.8	8.6	12.87	2.06	n.d.	n.d.	n.d.	0.225 ± 0.004	n.d. ± n.d.	n.d. ± n.d.	n.d. ± n.d.	n.d. ± n.d.
PACES 1-13	707122	5370884	337.9	22.87	86	6.0	8.9	0.69	2.86	n.d.	n.d.	n.d.	1.007 ± 0.012	n.d. ± n.d.	n.d. ± n.d.	n.d. ± n.d.	n.d. ± n.d.
TSAM-P1	706783	5379259	310.0	10.50	92	13.7	8.5	0.54	1.79	12.56	0.469	0.0318	1.193 ± 0.064	9.90 ± 0.03	0.0278 ± 0.0002	0.1854 ± 0.0006	294.5 ± 0.7
TSAM-P2	706782	5379258	310.6	16.46	128	12.2	8.3	1.03	2.37	15.38	0.576	0.0381	1.099 ± 0.022	9.86 ± 0.02	0.0276 ± 0.0002	0.1882 ± 0.0012	294.5 ± 0.7
TSSM-P1	705807	5370919	314.6	26.80	92	7.8	8.7	0.67	1.64	12.76	0.489	0.0337	1.117 ± 0.027	9.88 ± 0.03	0.0275 ± 0.0002	0.1865 ± 0.0009	294.7 ± 0.7
TSSM-P3	705166	5371107	309.1	27.61	96	6.3	8.9	4.54	2.00	13.73	0.520	0.0349	0.351 ± 0.014	9.85 ± 0.02	0.0278 ± 0.0001	0.1857 ± 0.0008	295.2 ± 0.9
TSSM-P5	707580	5370894	331.8	29.03	96	5.0	7.5	2.05	1.87	14.29	0.539	0.0374	0.709 ± 0.033	9.91 ± 0.02	0.0275 ± 0.0001	0.1873 ± 0.0006	293.7 ± 0.7
Barraute esker																	
Barraute municipality	747825	5369108	305.0	22.86	251	5.7	7.9	1.18	2.20	15.50	0.597	0.0408	0.935 ± 0.022	9.87 ± 0.02	0.0280 ± 0.0002	0.1874 ± 0.0010	293.6 ± 0.6
Harricana moraine																	
MDDEP-S	735432	5377299	375.1	41.76	226	13.1	8.3	0.54	2.02	15.10	0.596	0.0423	1.118 ± 0.025	9.85 ± 0.02	0.0277 ± 0.0002	0.1875 ± 0.0010	295.0 ± 0.8
MDDEP-P	716109	5375475	375.3	70.56	185	8.0	8.1	0.47	1.66	12.71	0.492	0.0341	1.207 ± 0.021	9.92 ± 0.02	0.0277 ± 0.0002	0.1880 ± 0.0010	296.5 ± 1.2
PACES 1-03	294017	5385992	375.0	64.40	115	6.5	8.4	0.55	1.89	n.d.	n.d.	n.d.	1.586 ± 0.018	n.d. ± n.d.	n.d. ± n.d.	n.d. ± n.d.	n.d. ± n.d.
Clay plain																	
Landrienne municipality	724345	5382191	318.0	89.60	351	6.4	7.1	1.24	2.80	17.47	0.653	0.0429	0.946 ± 0.024	9.84 ± 0.03	0.0281 ± 0.0002	0.1878 ± 0.0010	295.4 ± 0.7
55HB	714669	5377299	316.0	109.80	763	7.8	7.2	42.79	2.54	17.94	0.706	0.0473	0.224 ± 0.012	9.85 ± 0.02	0.0281 ± 0.0002	0.1896 ± 0.0009	294.8 ± 0.8
101CH	716109	5375475	302.0	35.05	527	8.0	7.8	2.34	2.70	18.16	0.709	0.0492	0.520 ± 0.019	9.84 ± 0.01	0.0277 ± 0.0002	0.1869 ± 0.0008	295.7 ± 0.7
Atmospheric value													1.000	9.77	0.0290	0.1880	295.5

Note: uncertainties on noble gas isotopic concentrations at University of Michigan (1σ) are ±1.5% (^{4}He), 1.3% (^{20}Ne), 1.3% (^{36}Ar), 1.5% (^{84}Kr) and 2.2% (^{132}Xe).
Uncertainties on ^{4}He and ^{20}Ne concentrations at University of Tokyo are (1σ) ±3%.
n.d. = not determined

Table 2
Aquifer and well physical parameters together with ^{3}H/^{3}He and U–Th/^{4}He ages.

Well name	Screen length (m)	Aquifer thickness z_0 (m)	Water table level m	Lithology at screen	Aquifer type	^{3}H TU	±	^{3}He$_{tri}$ TU	±	^{4}He$_{eq}$	^{4}He$_{ea}$	ΔNe (%)	Excess air cm^{3}STP × 10^{-3}	^{4}H$_{terr}$ cm^{3}STP g^{-1} × 10^{-8}	±	^{3}H/^{3}He age a	±	U–Th/^{4}He age a	±
Saint-Mathieu de Berry esker																			
Amos municipality	0.2	26.33	7.96	Gravel	–	12.72	1.05	33.68	1.48	4.52	0.13	2.18	0.24 ± 0.28	1.23	0.12	23.0	1.2	12.5	0.5
PACES 12-1	1.5	53.83	21.79	Sand	Unconfined	–	–	–	–					120.92	12.11	–	–	57.6	1.1
PACES 13-1	1.5	53.83	21.81	Sand	Unconfined	–	–	8.44	0.90					1.73	0.17	–	–	24.2	0.4
TSAM-P1	1.5	37.13	1.28	Sand, gravel	Confined	11.07	0.93	9.33	2.00	4.44	0.23	4.03	0.44 ± 0.30	0.70	0.07	10.9	1.9	62.4	2.0
TSAM-P2	1.5	37.13	1.59	Sand, gravel	Confined	13.14	1.03	23.45	1.67	4.56	1.80	23.66	3.44 ± 0.50	3.89	0.39	18.2	1.2	272.4	9.4
TSSM-P1	1.5	28.40	1.59	Sand, gravel	Confined	12.21	1.03	18.45	1.34	4.48	−0.37	−7.02	−0.70 ± 0.29	3.00	0.26	15.2	1.2	3.1	0.1
TSSM-P3	1.5	28.40	−1.00	Diamicton	Confined	3.10	0.04	15.73	7.74	4.50	0.72	11.29	1.38 ± 0.33	40.16	4.02	32.0	7.4	27.4	0.5
TSSM-P5	3.0	29.03	16.15	Diamicton	Confined	12.83	1.03	37.55	4.72	4.54	0.21	3.50	0.40 ± 0.45	15.76	1.58	24.3	2.0	10.5	0.2
Barraute esker																			
Barraute municipality	4.6	23.80	1.85	–	–	–	–	23.21	1.96	4.60	1.12	15.86	2.14 ± 0.39	6.06	0.61	–	–	64.8	2.7
Barraute municipality																		8.7	0.2
Harricana moraine																			
MDDEP-S	1.5	74.06	36.70	Sand, gravel	Unconfined	12.23	1.05	5.51	0.94	4.60	0.50	7.81	0.96 ± 0.25	0.34	0.03	6.6	1.1	121	9
MDDEP-P	1.5	74.06	36.51	Sand	Unconfined	11.49	0.95	9.87	0.80	4.47	−0.29	−5.46	−0.55 ± 0.22	0.82	0.05	9.9	0.9	41.0	1.9
PACES 1-03	1.5	74.06	36.57	Sand, gravel	Unconfined	–	–	21.76	0.92					0.76	0.08	–	–	91.0	4.9
								18.16	2.07										
Clay plain																			
Landrienne municipality	Unscreened	89.6	1.50	Basalt	Confined	–	–	18.16	2.07	4.64	2.99	33.13	5.70 ± 0.71	4.81	0.48	–	–	1473	292
55HB	Unscreened	97.3	7.25	Basalt	Confined	–	–	32.34	77.33	4.73	1.92	23.48	3.66 ± 0.60	421.21	42.17	–	–	137,000	28,000
101CH	Unscreened	10.7	–	Basalt	Confined	–	–	10.49	3.80	4.73	2.39	27.66	4.57 ± 0.44	16.23	1.62	–	–	207	6
101CH																		28	1

In UQAT and MDDEP wells, water for noble gas measurements was collected using a Waterra® Inertial Pump System which consists of a foot valve fixed at the bottom of a high-density polyethylene tube with a variable diameter of 5/8–1″ and an electric actuator pump Hydrolift-2®. In municipal wells, the water was collected directly at the wellhead. Water from domestic wells was collected at the closest water faucet, taking precautions to avoid intermediate reservoirs where the water could undergo degassing. Water was purged from wells and piezometers until measurement of main chemo-physical parameters (e.g., conductivity, pH, and temperature) stabilized. Water was subsequently allowed to flow through armored PVC tubes connected to a 14 cm³, 3/8″ diameter, refrigeration-type copper tube. After a few minutes the open tube was sealed using two steel clamps.

Water samples were measured for noble gas compositions at the Noble Gas Laboratory at the University of Michigan, except for three samples that were collected during the summer of 2012 (PACES 1-03, PACES 1-12 and PACES 1-13). Helium isotopic ratio was measured at Tokyo University. Water samples at University of Michigan were connected to a vacuum extraction system and noble gases were quantitatively extracted for inletting into a MAP-215-50 mass spectrometer. Extracted gases were passed over two Ti sponge getters to remove reactive gases, and sequentially allowed to enter the MAP-215-50 mass spectrometer using a cryogenic separator. The cryogenic separator temperatures were set at 35, 65, 200, 215, and 270 K for analysis of He, Ne, Ar, Kr, and Xe, respectively. The ^{4}He, ^{20}Ne and ^{40}Ar were measured using a Faraday detector while all other noble gas isotopes were measured using an electron multiplier in ion counting mode. During neon isotope analysis, a liquid N_2 cold trap was applied to minimize peak interferences and appropriate mass peaks were monitored to correct for interferences of ^{40}Ar^{++} and H_2^{18}O$^+$ on ^{20}Ne and $CO_2$$^{2+}$ on ^{22}Ne. The interference corrections for ^{20}Ne and ^{22}Ne were typically ∼1.1% and 0.17%, respectively. Before each sample analysis, a calibrated amount of air standard was analyzed following the same procedure as the sample measurement for checking sensitivity of the MAP215-50 mass spectrometer. The blank correction was applied to all measured peaks, but was negligible. Isotopic abundances for each sample were normalized to the air standard after blank correction. Elemental abundances of ^{4}He, ^{22}Ne, ^{36}Ar, ^{84}Kr, and ^{132}Xe have typical uncertainties of 1.5%, 1.3%, 1.3%, 1.5% and 2.2%, respectively and all uncertainties are at ±1σ level. Additional details on the noble gas analytical procedure at University of Michigan can be found in Ma et al. (2005).

The three samples collected in summer 2012 (PACES-03, PACES 1-12 and 1-3; Table 1) were analyzed at the Atmosphere and Ocean Research Institute (AORI) at the University of Tokyo for helium isotopes and ^{20}Ne. These samples were degassed offline using a dedicated line evacuated with a turbo-molecular pump. Extracted gas was collected in a lead-rich glass ampoule. The ampoule was connected to a stainless steel line for purification on a Ti-getter and cryogenic separation of He from other noble gases. The helium aliquot was then analyzed for the ^{3}He/^{4}He isotopic ratio using a Helix SFT calibrated against the HESJ standard (Helium Standard of Japan; Matsuda et al., 2002). Precision on the ^{3}He/^{4}He ratio of HESJ is typically ±0.2% (2σ) (Sano et al., 2008). Prior to being cryogenically adsorbed, the amount of ^{4}He and ^{20}Ne was measured on a Pfeiffer QMS Prisma™ 80 connected to the preparation line with a typical precision of ±3% (1σ).

Water samples for tritium (^{3}H) analysis were collected using 1 L Nalgene® bottle filled up to prevent degassing and sealed before shipment to the Environmental Isotopes Laboratory (EIL) of the University of Waterloo. Liquid scintillation counting (LSC) is the technique used by EIL for quantification of tritium. Samples being analyzed for tritium are concentrated 15 times by electrolysis and subsequently counted. Detection limit for enriched samples is 0.8 TU (Heemskerk and Johnson, 1998).

To calculate radiogenic ^{4}He production rates from the sediments of the aquifers, U and Th were measured by neutron activation at the Slowpoke Laboratory of the University of Montreal, in sediments and rock fragments from the top of the Harricana moraine, a few tens of meters from the position of MDDEP-S and -P wells (Fig. 1a). U and Th concentrations ranged from 0.2 to 0.84 ppm and from 0.34 to 3.52 ppm, respectively.

4. Results

Table 1 reports the concentrations of major noble gas isotopes (^{4}He, ^{20}Ne, ^{36}Ar, ^{84}Kr and ^{132}Xe) and He, Ne and Ar isotopic ratios except for the three samples analyzed at the University of Tokyo for which only He isotopes and ^{20}Ne were measured. ^{4}He concentrations range from 4.7 to 5.5 × 10^{-8} cm³STPg^{-1}, values that are close to the concentration at solubility equilibrium with the atmosphere (ASW or Air Saturated Water; Smith and Kennedy, 1983), to 4.28 × 10^{-6} cm³STP/g^{-1} which was measured in groundwater collected from the deepest well in the fractured bedrock aquifer (55 HB; Fig. 1; Table 1). Measured ^{3}He/^{4}He ratios (R) normalized to that of the atmosphere (Ra = 1.386 × 10^{-6}; Lupton, 1983) range from 1.849 ± 0.036 times (Amos municipality well) to 0.224 ± 0.012 times the atmospheric ratio (55HB; Table 1).

^{20}Ne/^{22}Ne ratios in most samples are slightly higher than the atmospheric value of 9.768 (Sano et al., 2013) (9.83 < ^{20}Ne/^{22}Ne < 9.91), but are inversely correlated with ^{40}Ar/^{36}Ar ratios, which vary between 294.4 and 296.5 (Table 1) (atmospheric value is 295.5; Ozima and Podosek, 1983), indicating mass-dependent fractionation of Ne and Ar of atmospheric composition (Marty, 1984). The ^{38}Ar/^{36}Ar ratios range from 0.1854 to 0.1896 (atmospheric value of 0.1880; Ozima and Podosek, 1983) and do not display a correlation with the ^{40}Ar/^{36}Ar ratios. Kr and Xe isotopic compositions are entirely atmospheric and they have been not reported.

Table 2 reports technical specifications of the sampled wells (e.g., depth, screen length, and aquifer thickness), calculated helium components dissolved in water (^{4}He$_{eq}$, ^{4}He$_{ea}$, ^{4}He$_{terr}$ and ^{3}He$_{tri}$) and measured tritium content (^{3}H in TU, corrected of the time interval between ^{3}He$_{tri}$ and ^{3}H analyses), which are needed for calculating apparent ^{3}H/^{3}He ages and U–Th/^{4}He ages (see discussion). ^{4}He$_{eq}$ is the dissolved helium in solubility equilibrium with the atmosphere (^{4}He$_{eq}$). ^{4}He$_{ea}$ is the atmospheric helium in excess of the solubility equilibrium concentration. The latter, known as the "excess air component" result from air bubbles entering the water table and dissolved in groundwater (Heaton and Vogel, 1981). ΔNe (%) ([Ne]$_{measured}$/[Ne]$_{atmospheric\ equilibrium}$ − 1) × 100 expresses the total amount of excess air (Table 2; Aeschbach-Hertig et al., 2001). These parameters ($_4$He$_{eq}$, ^{4}He$_{ea}$ and ΔNe (%); Table 2) have been estimated from calculation of Noble Gas Temperatures (NGT) based on Ne, Ar, Kr and Xe concentrations in groundwater and applying the UA (Unfractionated Air) model of excess air incorporation in groundwater (Stute and Schlosser, 1993) through an error-weighted, nonlinear inverse technique (Ballentine and Hall, 1999).

The ^{4}He$_{terr}$ is the terrigenic helium produced by U and Th decay in Earth's crust or derived from the mantle and it is calculated as ^{4}He$_{terr}$ = ^{4}He$_{tot}$ − (^{4}He$_{eq}$ + ^{4}He$_{ea}$), where ^{4}He$_{tot}$ is the total initial amount of helium, as reported in Table 1. Finally, tritiogenic ^{3}He derived from decay of post-bomb tritium in young water (^{3}He$_{tri}$) has been calculated using the equation (Schlosser et al., 1989):

$$^3He_{tri} = {}^4He_{tot} \cdot (R_{tot} - R_{terr}) - {}^4He_{eq} \cdot (R_{eq} - R_{terr}) - \left(\frac{^4He}{^{20}Ne}\right)_{ea}$$

$$\cdot \left({}^{20}Ne_{tot} - {}^{20}Ne_{eq}\right) \cdot (R_{ea} - R_{terr}) \qquad (1)$$

where $\ll R \gg$ refers to the ^{3}He/^{4}He ratio. R_{tot} is the measured ^{3}He/^{4}He ratio. R_{ea} is the ^{3}He/^{4}He ratio for the "excess air" component and it is assumed to be atmospheric ($R_{ea} = R_{atm} = 1.386 \times 10^{-6}$; Lupton, 1983). R_{eq} is the ^{3}He/^{4}He ratio at ASW condition and it is equal to $\alpha * R_{atm}$ (1.36×10^{-6}) with α representing the fractionation factor of 0.983 (Benson and Krause, 1980). R_{terr} corresponds to the time-integrated ^{3}He/^{4}He ratio from ^{3}He and ^{4}He crustal production. Finally, the $(^4$He/^{20}Ne$)_{ea}$ ratio of the "excess air" component is also assumed to be atmospheric and equal to 0.3185.

5. Discussion

5.1. Helium component separation

Helium components dissolved in Amos groundwater can be visualized in a Weise-plot (Weise and Moser, 1987; Fig. 2). In this plot, the excess-air-corrected helium isotopic ratio ((^{3}He$_{tot}$–^{3}He$_{ea}$)/ (^{4}He$_{tot}$–^{4}He$_{ea}$)) is plotted versus the ratio between the He$_{eq}$ concentration and the normalized excess-air-corrected helium concentration (^{4}He$_{eq}$/(^{4}He$_{tot}$–^{4}He$_{ea}$)). In the following discussion, as well as Fig. 2, all ^{3}He/^{4}He values (R) have been normalized to R_{atm} (1.386×10^{-6}). Addition of ^{3}He$_{tri}$ will shift the (^{3}He$_{tot}$–^{3}He$_{ea}$)/ (^{4}He$_{tot}$–^{4}He$_{ea}$) ratio up from its initial ASW isotopic composition at the recharge (R_{eq}; Fig. 2). Addition of ^{3}He$_{terr}$ produced by nucleogenic reactions with Li (Morrison and Pine, 1955) and ^{4}He$_{terr}$ from α-decay of U and Th in crustal rocks will shift ratios to the lower left corner of the plot with a ^{4}He$_{eq}$/(^{4}He$_{tot}$–^{4}He$_{ea}$) value of zero (i.e., containing only ^{4}He$_{terr}$) and a R_{terr} value corresponding to the time-integrated ratio from ^{3}He and ^{4}He crustal production (typically 0.02–0.03Ra; e.g., Andrews and Lee, 1979). Mixing between the different end-members will be represented by a straight line of equation $Y = mX + b$ (e.g., Stute et al., 1992):

$$\underbrace{\frac{(^3He_{tot} - ^3He_{exc})}{(^4He_{tot} - ^4He_{exc})}}_{Y} = \underbrace{\left(R_{eq} - R_{terr} + \frac{^3He_{tri}}{^4He_{eq}} \right)}_{m} \cdot \underbrace{\frac{^4He_{eq}}{^4He_{tot} - ^4He_{exc}}}_{X} + \underbrace{R_{terr}}_{b}$$
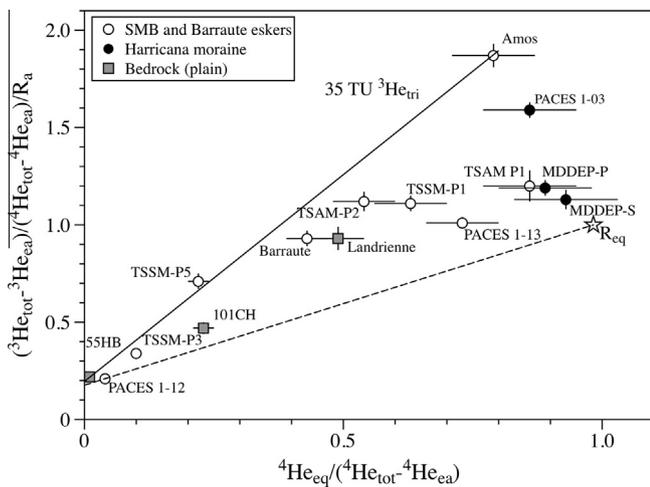
(2)

Fig. 2. Weise-plot for groundwater samples from Saint-Mathieu–Berry (SMB) and Barraute eskers (white dots); from Harricana moraine (black dots) and from the fractured aquifer under the clay plain (gray squares). The dashed line represents the mixing line between water containing atmospherically derived helium at air saturated water conditions or ASW (^{3}He/^{4}He ratio = R_{eq} = 0.983Ra) and water enriched in terrigenic helium, represented by the helium composition of sample PACES 12-1. The plain line represents the mixing between water containing 35 TU ^{3}He$_{tri}$ (equivalent to 8.47×10^{-14} cm^{3}STP g^{-1} of ^{3}He$_{tri}$) mixed with water enriched in terrigenic helium ^{4}He, here represented by the helium composition of sample 55HB.

All groundwater samples plot between two mixing lines (Fig. 2). The first passes through the ASW end-member (R_{eq}) and the sample PACES 12-1. The Y-intercept of this mixing line (corresponding to R_{terr}) is 0.1765. The second mixing line passes through the waters of Amos municipality, TSSM-P5 and 55HB wells with a Y-intercept of 0.2198. This straight line corresponds to a groundwater containing 35 TU tritiogenic ^{3}He mixed with an older groundwater enriched in terrigenic helium. For $X = 0$ term "b" of Eq. (2), we assumed an average (±std dev) R_{terr} value of 0.198 ± 0.031.

The obtained R_{terr} value is higher than the expected crustal value of 0.02–0.03Ra and clearly denotes the presence of ^{3}He$_{terr}$ excesses. These ^{3}He$_{terr}$ excesses could be caused either by the addition of 2.4% of mantle helium to the groundwater or from an enhanced contribution of nucleogenic ^{3}He from lithium decay in crustal rocks. Production of the R_{terr} with a value of 0.2Ra by *in situ* nucleogenic processes would require reservoir rocks to contain Li concentrations between 600 and 2200 ppm, depending on U and Th concentrations in these same rocks (Andrews and Lee, 1979). These lithium concentrations, not unusual in this area, are far greater than the average upper crust value of 20 ppm (Ballentine and Burnard, 2002). The crystalline basement underneath the eskers contains pegmatite intrusions known to be very rich in lithium. For example, 20 km southeast of the SMB esker (area of Mont Video, see Fig. 1a), Canada Lithium Corp. has carried out a feasibility study for mining carbonate phases in a pegmatitic intrusion containing up to 1.2 wt.% (12,000 ppm) lithium (http://www.canadalithium.com/fr/QuebecLithium.asp). Thus, we cannot exclude that groundwater flowing through the crystalline basement underneath the eskers has interacted with these Li-rich ore bodies, charging them with ^{3}He$_{terr}$.

Fig. 2 shows that groundwater flowing in eskers and in the clay plain contains a mixture of ^{3}He$_{tri}$ and terrigenic helium. It is possible to take advantage of these helium components to estimate groundwater residence times and to reconstruct the age of esker aquifers using both the ^{3}H/^{3}He (e.g., Tolstikhin and Kamenskiy, 1969; Takaoka and Mizutani, 1987) and U–Th/^{4}He dating methods (e.g., Torgersen and Clarke, 1985).

5.2. ^{3}H/^{3}He apparent groundwater ages

Natural background of tritium (^{3}H) is derived from spallation reactions with N in the troposphere. This relatively low background has undergone a remarkable change during the 60s. Indeed, fallout of anthropogenic tritium from atmospheric nuclear weapon tests conducted to a peak record of tritium content in precipitation during this period (e.g., Clark and Fritz, 1997). Tritium has been normally used, coupled to tritium records in precipitation, to estimate groundwater age. Nevertheless, since tritium is returned to its natural background, the exact time of ^{3}H delivery to the aquifer is difficult to well evaluate based only on the initial tritium concentration. Thus, since ^{3}He is produced by tritium decay with a half-life ($T_{1/2}$) of 12.32 ± 0.02 years (Lucas and Unterweger, 2000), the coupled measurements of these two elements can be useful to partially remedy to this problem. Indeed, it has the advantage to be independent of the initial tritium concentration of the water sample. If the amount of ^{3}H and ^{3}He$_{tri}$ are measured, the ^{3}H/^{3}He apparent age (t) can be calculated using the following equation:

$$t = \frac{T_{1/2}}{\ln 2} \cdot \ln \left(1 + \frac{^3He_{tri}}{^3H} \right)$$

(3)

The main difficulty and source of uncertainties in the calculated ^{3}H/^{3}He groundwater age is the separation of ^{3}He$_{tri}$ from the other helium components ("ea", "terr" and "eq"), which is addressed using Eq. (1). Uncertainties in ^{3}H/^{3}He apparent were calculated as propagated error, which takes into account all the uncertainties

for each variable used in Eqs. (1) and (3). The total uncertainty of the $^3H/^3He$ ages ranges from 5.3% (Amos) to 23% (TSSM-P3) of the calculated age. The source of the larger uncertainty in the $^3H/^3He$ ages of TSSM-P3 derives from the poor fitting to the UA model with consequent larger uncertainties in the calculated "eq" and "ea" helium components (Table 2). The youngest $^3H/^3He$ ages were measured for the Harricana moraine (6.6 ± 1.1 a for MDDEP-S and 9.6 ± 0.9 a for MDDEP-P) while the SMB esker groundwater showed older apparent $^3H/^3He$ ages from 10.9 ± 1.9 a (TSAMP-1) to 32.0 ± 7.4 a (TSSM-P3) (Table 2 and Fig. 1b).

The calculated $^3H/^3He$ ages are valid if one assumes that the tracer traveled from the recharge area to the well without hydrodynamic dispersion or mixing, i.e., following a *piston flow* (*PFM*) behavior. This is the case for tracers measured from shallow, short-screened monitoring wells in unconfined aquifers with a small recharge area or confined aquifers, as it is the case for the shallower SMB and Harricana wells (Table 2). We cannot rule out dispersion or water mixing, in particular for the deeper wells or the Amos municipality well, which is a horizontal multi-drain well with long screens. Binary mixing is certainly occurring in the eskers as indicated by the presence of tritiogenic ^3He and radiogenic ^4He in the same water parcel (Fig. 2). An important limiting case is the addition of pre-bomb water virtually free of tritium. This water will dilute both tritium and $^3He_{tri}$ with very small effects on the ratio and thus on the calculated age.

The $^3H/^3He$ ages formally calculated from Eq. (3) are "apparent" ages. Indeed it might be affected by mixing and dispersion, which makes complicated their quantitative interpretation. To test whether or not calculated $^3H/^3He$ apparent ages have been significantly affected by mixing or hydrodynamic dispersion, we compared the reconstructed initial tritium content ($^3H_{init} = ^3H + ^3He_{tri}$) with its historical record in precipitation at the closest station to Amos, i.e. Ottawa (Fig. 3; IAEA/WMO, 2004b). With the exception of TSSM-P3 artesian well, all samples fit well with the average tritium input curve. TSSM-P3 falls below the mean monthly input curve and can be explained by a binary mixing with pre-bomb water (Aeschbach-Hertig et al., 1998). The dashed curve in Fig. 3 represents a two-component mixture of 30% of water recharged
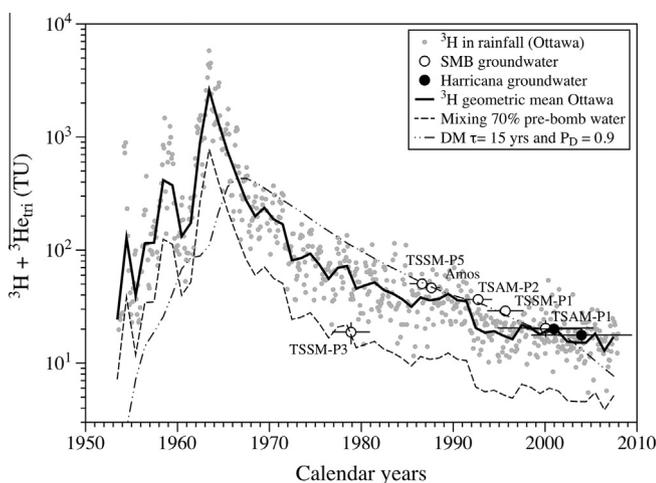
during a single year within the observed period and 70% of pre-bomb water. It is worth noting that sample TSSM-P3 is the one containing the most radiogenic ^4He, among those which ^3H has been measured (Table 1). Although the other SMB and Harricana wells plot close to the average tritium input curve, they could also be affected by dispersion (Fig. 3). The dash-double dotted curve represents the isotopic signal smoothed by dispersion using a scenario with a mean residence time τ of 15 years and a dispersion coefficient P_D of 0.9. The curve was obtained by using a modified version of the software BOXMODEL (Kinzelbach et al., 2002) that we adapted to the reference tritium precipitation curve of Ottawa. However, this is not a unique solution and several other curves can be plotted using different residence time τ and dispersion coefficient P_D. This situation underlies the limitation of using such a plot for data fitting very closely to the mean annual tritium rainfall curve (e.g., Aeschbach-Hertig et al., 1998).

To understand if our hydrological system can be approximated to *PFM*, we plotted the apparent $^3H/^3He$ ages versus the distance below the water table (Fig. 4). Three well nests can be distinguished geographically in the area (Fig. 1b), and for which $^3H/^3He$ ages have been calculated (Table 2): Amos municipality, TSAM-P1 and TSAM P2 tapping water in the same aquifer in the northern part of the SBM esker; TSSM-P1 and -P3 in the central western flank of the SMB esker; and the two wells MDDEP-S and MDDEP-P drilled at different depths on the top of the Harricana moraine (Fig. 1a). Well TSSM-P5 is tapping water from the same aquifer than TSSM-P1 and P3 but is located on the other flank of the SMB esker. The low water table measured in this well (−16 m against 1.5 m for the other two wells; Table 2) indicates likely that flow is directed from the center of the esker toward its flanks (Riverin, 2006), following two distinct hydraulic gradients.

If these wells are intercepting a water system that reproduces a *PFM* behavior in an unconfined aquifer and in which recharge is spatially uniform, then a simple logarithmic relationship exists between the $^3H/^3He$ ages (t) and the vertical velocity (V_0) at the water table (Vogel, 1967):

$$V_0 = \frac{z_0}{t} \ln\left(\frac{z_0}{z_0 - z}\right) \tag{4}$$

where z_0 is the thickness of the aquifer (m) and z the distance below the water table. It is apparent that the age profile obtained for well
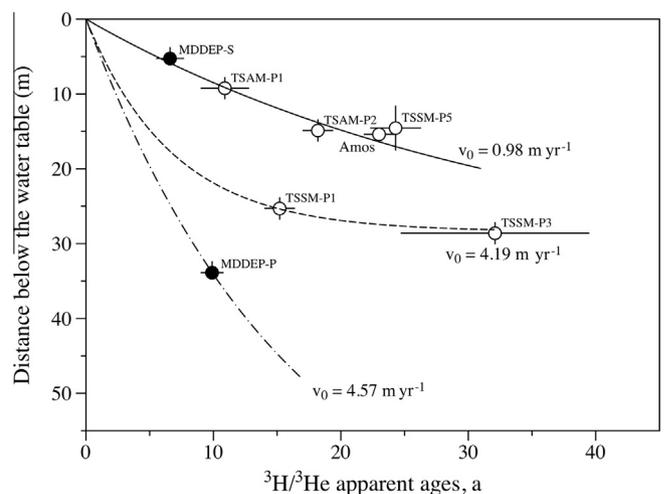

Fig. 3. Comparison of the initial tritium content ($^3He_{init} = ^3H + ^3He_{tri}$) of the groundwater samples against the tritium record in rainfall (gray dots) recorded at the IAEA Ottawa station (IAEA/WMO, 2004b; data: http://www-naweb.iaea.org/napc/ih/IHS_resources_isohis.html). The plain line represents the monthly-averaged Ottawa tritium rainfall curve, reported as reference. The dashed line below the Ottawa ^3H reference curve represents a two-component mixture of 30% of water recharged during a single year within the observed period and 70% of ^3H-depleted pre-bomb water. The dash-double dotted curve above the Ottawa ^3H reference curve represents the tracer isotopic signal smoothed by hydrodynamic dispersion. Symbols are as in Fig. 2.

Fig. 4. Groundwater $^3H/^3He$ apparent ages plotted against the depth of the sampled wells of SMB esker and Harricana moraine. Plain and dotted lines represent the simulated groundwater ages following the Vogel (1967) model, fitting the experimental data by adjusting the vertical velocity (V_0) (see text for details). Symbols are as in Fig. 2.

nests TSAM-P1, -P2 and Amos municipality can be fitted rather well by extrapolating the travel time (t) from Eq. (4). This leads to a vertical velocity of 0.98 m yr^{-1} (Fig. 4), using an average aquifer thickness of 33.5 m (Table 2). Using the aquifer thickness z_0 and distance below the water table z calculated for each of these three wells individually leads to, the following vertical velocities V_0: 0.97 m yr^{-1} for TSAM-P1, 1.04 m yr^{-1} for TSAM-P2, and 1.00 m yr^{-1} for Amos. Well nests TSSM-P1 and -P3 age profiles fit also well for a vertical velocity V_0 of 4.18 m yr^{-1} and an aquifer thickness of 28.4 m, though larger uncertainties must be considered for these numbers taking into account those on the TSSMP-3 ^{3}H/^{3}He age (Table 2). Finally, the deeper MDDEP-P well requires V_0 = 4.75 m yr^{-1} (Fig. 4) for a aquifer thickness of 74 m. Shallower wells MDDEP-S and TSSM-P5 are close to the age profile of well nests TSAM-P1, -P2 and Amos, suggesting similar vertical velocities. These have been estimated at 0.83 m yr^{-1}.

To test whether the calculated velocities for the shallower wells are plausible and the apparent ^{3}H/^{3}He ages can be confidently assumed to be close to actual *PFM* residence time, the expected recharge rate (r) was calculated using the following relationship (Solomon et al., 1993):

$$r = V_0 \cdot \phi \tag{5}$$

where V_0 is the vertical velocity (as calculated from Fig. 4) and ϕ is the aquifer effective porosity (25–30%). The resulting recharge rates for the shallower wells (V_0 = 0.98 m yr^{-1}; Fig. 4) range from 245 mm yr^{-1} to 294 mm yr^{-1}, a range of values that agrees well with average recharge rates of 222–306 mm yr^{-1} calculated through hydraulic balance considerations (Cloutier et al., 2013). In contrast, recharge rates calculated for the deeper wells TSSM-P1, TSSM-P3 (V_0 = 4.19 m yr^{-1}) and MDDEP-P (V_0 = 4.57 m yr^{-1}) range from 1047–1257 to 1142–1371 mm yr^{-1}, a range of values which exceeds the total recharge input, estimated between 854 and 930 mm yr^{-1} (Cloutier et al., 2013). For the deeper wells, groundwater flow probably deviates from the *PFM* with dispersion effects or ^{3}He diffusive loss that render apparent ^{3}H/^{3}He ages younger than the real ones. It is worth noting that Riverin (2006) suggested the presence of two types of flow in the southern part of the SMB esker, close to wells TSSM-P1, P3 and P5, one longitudinal to the axis of the esker and the other transversal. This situation can favor the occurrence of turbulence and some dispersive effect due to mechanical mixing when the mainstream is divided into several water flow components.

5.3. U–Th/^{4}He ages of the older water component

Measured groundwater samples contain a small amount of terrigenic ^{4}He (3.36×10^{-9}–4.21×10^{-6} ccSTP g$_{H_2O}$; Table 2). Higher terrigenic ^{4}He amounts are present in wells tapping water from the fractured basement beneath the clay plain (55HB and 101CH; Fig. 2) or in the deeper wells of the SMB esker (PACES 1-12 and TSMP-3) in contact with the basement or the basal till.

In the absence of an external mantle source, terrigenic ^{4}He is exclusively produced from α-decay of U and Th in the aquifer rocks and subsequently released into the water (e.g., Andrews and Lee, 1979). To explain the presence of this radiogenic helium component, we can assume that (i) groundwater is recent (^{3}H/^{3}He ages reflect the average residence time of water) and accumulate ^{4}He *in situ*, i.e., from a source internal to the aquifer (e.g., Solomon et al., 1996); or (ii) esker groundwater is a mixture of two water components, one tritiated freshwater recharged recently in the system (6–32 years old) and an older pre-bomb groundwater component which has accumulated large amounts of terrigenic ^{4}He. This older component could reside either in the esker aquifer, possibly in the less permeable and conductive basal glacial till (though its presence is limited to the well TSSMP3 and -P5, southern part of

SMB; Cloutier et al., 2013 and Table 2) or just below, in the basal fractured bedrock aquifer.

If the first hypothesis is correct, we can then calculate the *in situ* production rate of ^{4}He (P$_{4He}$ in cm^{3}STP g$_{rock}^{-1}$ yr^{-1}), extrapolating it from the U–Th/^{4}He age equation of Torgersen and Clarke (1985):

$$P_{4He} = \frac{[^4He_{terr}]}{t \cdot \Lambda_{4He} \cdot \left(\frac{1-\phi}{\phi}\right) \cdot \rho_{rock}} \tag{6}$$

where (^{4}He$_{terr}$) is the measured radiogenic ^{4}He concentration in groundwater (cm^{3}STP g^{-1}); Λ_{4He} thickness of the aquif is the He retention factor (^{4}He$_{released}$/^{4}He$_{produced}$), taken as 1 (Sano et al., 1998); $(1 - \phi/\phi)$ is the void ratio where ϕ is the effective porosity in %, assumed equal to 25–30%; and ρ is the aquifer matrix density (assumed to be 2.65 gcm^{-3}). The term "t", the accumulation time is here assumed equal to the calculated ^{3}H/^{3}He ages (Table 2).

Results show that the P$_{4He}$ should range between 6.40×10^{-11} and 2.03×10^{-9} cm^{3}STP g$_{rock}^{-1}$ yr^{-1}. These helium production rates are 480–15,000 times higher than that expected from *in situ* production from the U and Th content measured in the aquifer matrix, i.e., $1.33 \pm 0.64 \times 10^{-13}$ cm^{3}STP g$_{rock}^{-1}$ yr^{-1}. This latter has been calculated using the production equation (Andrews and Lee, 1979):

$$P_{4He} = 1.1 \times 10^{-13}[U] + 2.88 \times 10^{-14}[Th] \tag{7}$$

where [U] and [Th] are concentrations (ppm). Here we used U and Th concentrations from 0.2 to 0.84 ppm and from 0.34 to 3.52 ppm, as measured by neutron activation in glaciofluvial rock samples collected in the area. Pinti et al. (2011) calculated a higher P$_{4He}$ for the Superior Province magmatic and metamorphic rocks that mainly constitute the esker aquifer matrix (6.41×10^{-13} cm^{3}STP g$_{rock}^{-1}$ yr^{-1}). This production rate is undistinguishable from that of the upper continental crust (6.43×10^{-13} cm^{3}STP g^{-1} yr^{-1}; Ballentine and Burnard, 2002). Using a production rate of 6.41×10^{-13} cm^{3}STP g$_{rock}^{-1}$ yr^{-1}, the measured amount of terrigenic ^{4}He in the SMB and Harricana groundwater is still 100–3000 times higher than the U–Th *in-situ* production.

Solomon et al. (1996) carried out helium diffusion experiments on aquifer rocks of Sturgeon Falls, Ontario, and on an esker composed of volcano-metamorphic rock debris of the Canadian Precambrian Shield, thus similar to the SMB esker and the Harricana moraine. They showed that old protoliths of these Precambrian rocks release ^{4}He at rates greater than those supported by steady-state U–Th production. The resulting apparent production rate for the rocks composing the Sturgeon Falls aquifer would be 300 times greater than that expected from U and Th decay, i.e., 7.5×10^{-11} cm^{3}STP g$_{rock}^{-1}$ yr^{-1} (Solomon et al., 1996). This value is close to our lower estimates of the P$_{4He}$ (6.40×10^{-11} cm^{3}STP g$_{rock}^{-1}$ yr^{-1}). However, in order to account for the higher amounts of terrigenic ^{4}He found in the Amos area, a ^{4}He production rate of 2.03×10^{-9} cm^{3}STP g$_{rock}^{-1}$ yr^{-1}, is required, i.e., two order of magnitude higher than that found at Sturgeon Falls (Solomon et al., 1996).

Although an internal source of radiogenic helium is an appealing hypothesis to be confirmed through helium diffusion experiments, it is likely that terrigenic helium is introduced in the eskers by an upward flux entering the base of the aquifer. Fig. 5(a–d) shows the ^{4}He$_{terr}$ and the R/Ra ratio against the depth of the sampled well and the water salinity (TDS in mg L^{-1}; Table 1). It is clear that the ^{4}He$_{terr}$ amount increases with depth, creating two distinct concentration gradients (Fig. 5a): one including all the SMB water samples and one from the fractured bedrock (101CH); the other including the samples from the fractured bedrock 55HB and Landrienne and those from the Harricana Moraine (PACES 1-03, MDDEP-P and -S). In the SMB, the helium gradient
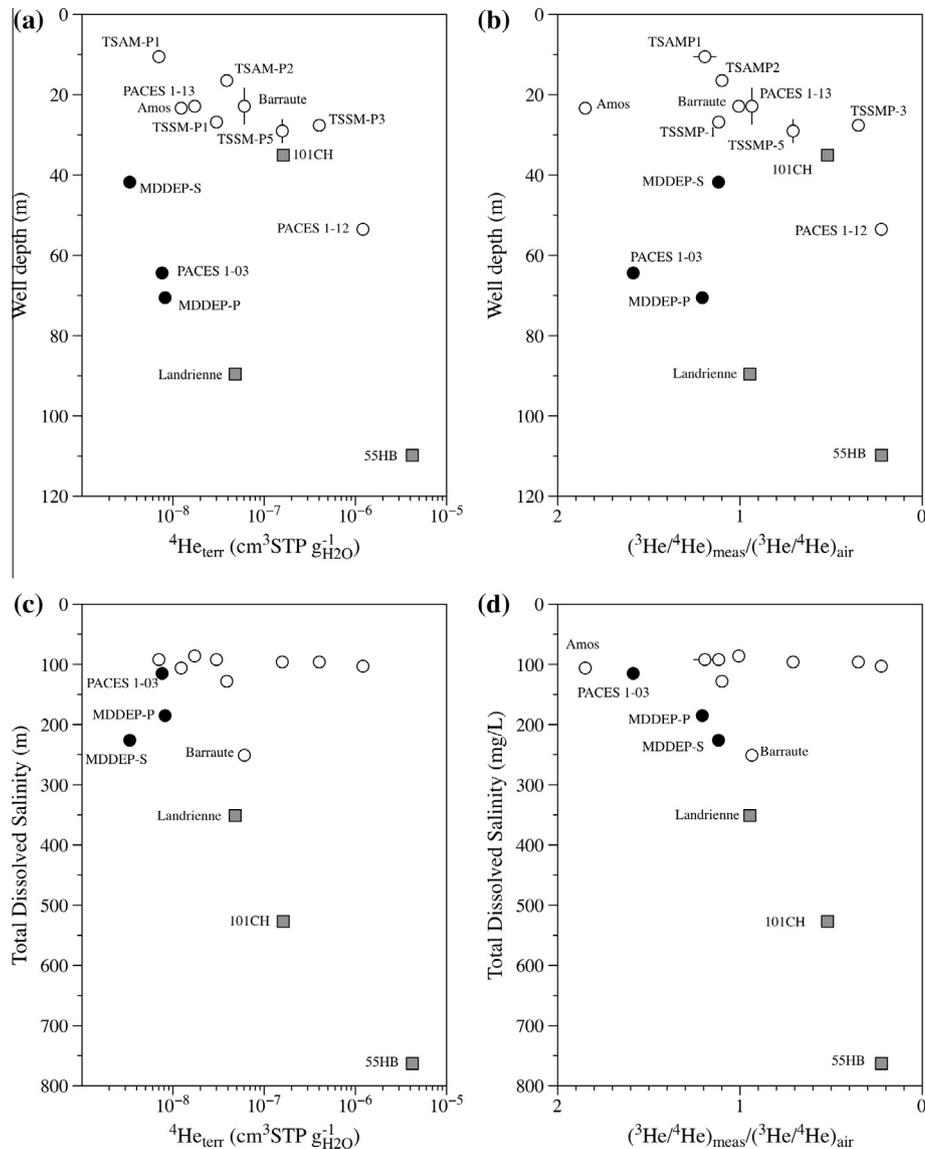
Fig. 5. Helium concentration and helium isotopic (^{3}He/^{4}He) gradients versus the depth of sampled wells (a–b) and the total dissolved salinity (TDS) of groundwater (c–d). Symbols are as in Fig. 2.

can be interpreted as upward flux of helium progressively diluted and dispersed by flowing freshwater essentially depleted in ^{4}He$_{terr}$, but which contains a ^{3}He$_{tri}$ component (Fig. 5b). In the case of the Harricana moraine, the terrigenic ^{4}He concentration gradient is accompanied by a salinity gradient suggesting that helium is transported in slightly saline water phase up into the moraine, where helium and salinity inputs are subsequently diluted by freshwater. The source of salt is groundwater located in the fractured bedrock under the clay plain (55HB and 101CH; Table 1) (Figs. 5c–d).

In order to quantify both flux from below and accumulation of ^{4}He$_{terr}$ in a confined aquifer, Torgersen and Ivey (1985) proposed a simple model assuming that steady-state flow and transport is reached in the system. The advection–dispersion equation describing their model is given by:

$$v_x \frac{\partial C}{\partial x} + D_T \frac{\partial^2 C}{\partial z^2} = P \qquad (8)$$

where v_x is the horizontal flow velocity, C is the ^{4}He$_{terr}$ concentration, x is the distance from the recharge, z is the relative vertical position inside the aquifer, D_T is the coefficient of hydrodynamic

transverse dispersion (Freeze and Cherry, 1979) that take into account the vertical dispersivity and the molecular diffusion of the solute (here ^{4}He$_{terr}$) in the porous medium. P is a source term and in our case it represents the accumulation of ^{4}He in the water resulting from *in situ* production $P_{^4He}$. The prescribed boundary conditions for this model are (1) a ^{4}He$_{terr}$ concentration that initially is zero for all depths in the aquifer; and (2) a constant flux J_0 of ^{4}He$_{terr}$ entering the aquifer across the bottom boundary z_0. Torgersen and Ivey (1985) gave the analytical solution of the differential Eq. (7):

$$C = Pt + \frac{J_0 t}{z_0 \rho \phi}$$
$$+ \frac{J_0 t_0}{D_T \rho \phi} \left[\frac{3\left(\frac{z}{z_0}\right) - 1}{6} - \frac{2}{\pi^2} \sum_{m=1}^{\infty} \frac{(-1)^m}{m^2} \exp\left(-\frac{D_T m^2 \pi^2 t}{z_0^2}\right) \cos\left(\frac{m\pi z}{z_0}\right) \right] \qquad (9)$$

where z_0 is the thickness of the aquifer, ρ is the water density, ϕ is the porosity, J_0 is the upward ^{4}He flux entering the bottom of the confined aquifer, and t is the groundwater age. Because the exact recharge distance of SMB and Harricana wells is not well known,

we calculated the $^4\text{He}_{terr}$ concentrations (C) and present them as a function of $^3\text{H}/^3\text{He}$ groundwater ages (t) (Fig. 6a–d).

It is worth noting that there is a logarithmic correlation between the $^3\text{H}/^3\text{He}$ ages and the concentration of $^4\text{He}_{terr}$ (Fig. 6a–f), as observed in several other aquifers (e.g., Castro et al., 1998, 2000; Castro and Goblet, 2005; Ma et al., 2005). This correlation indicates that the accumulation of $^4\text{He}_{terr}$ in the aquifer is a function of the water residence time. Further, for each well nest identified above (Amos, TSAM-P1 and P2; TSSM-P1, -P3, -P5; MDDEP-S and -P), the higher $^4\text{He}_{terr}$ concentrations are found in the deeper wells, i.e., wells approaching the bottom of the aquifer ($z/z_0 \to 1$; Fig. 6a–f). This observation supports the hypothesis of an external upward ^4He flux entering the bottom of the aquifer (Fig. 5a).

Simulated $^4\text{He}_{terr}$ fluxes using Eq. (8) were calculated using z and z_0 data from Table 2. D_T was assumed equal to 0.13 $\text{m}^2 \text{yr}^{-1}$. This value has been obtained from measurements of transverse dispersion performed in homogeneous sandstone (Freeze and Cherry, 1979) and it is roughly constant for a wide range of velocities (varying from 0.32 to 16 m yr^{-1}; Castro et al., 2000). Simulation results are reported for the well nest Amos, TSAM-P1 and -P2, the nest composed of TSSAM-P1, P3 and P5 and the nest MDDEP-S and -P (Fig. 6a–f). Simulations were carried out for porosity values varying from 25% to 30%, which give us a minimum and maximum $^4\text{He}_{terr}$ flux J_0 estimate for each well nest. $^4\text{He}_{terr}$ fluxes range from 8.0–8.5×10^{-8} $\text{cm}^3\text{STP cm}^{-2} \text{yr}^{-1}$ (Fig. 6a–b) to 5.8–6.6×10^{-7} $\text{cm}^3\text{STP cm}^{-2} \text{yr}^{-1}$ (Fig. 6c–d) in the SMB esker. Much lower $^4\text{He}_{terr}$ fluxes, on the order of 2.0–2.7×10^{-8} $\text{cm}^3\text{STP cm}^{-2} \text{yr}^{-1}$, are derived for the Harricana moraine due to dilution by freshwater as mentioned earlier (Fig. 6e–f).

Calculated ^4He fluxes are 5–165 times lower than the average helium continental crustal flux of 3.3×10^{-6} $\text{cm}^3\text{STP cm}^{-2} \text{yr}^{-1}$ (O'Nions and Oxburgh, 1983) and even lower if compared to the helium flux from the Canadian Precambrian Shield (5.83×10^{-6}-$\text{cm}^3\text{STP cm}^{-2} \text{yr}^{-1}$; Torgersen, 2010). Helium fluxes similar to those estimated for the Amos region are present in shallow aquifers of the Paris Basin (Castro et al., 1998; Marty et al., 1993), Austria Molasse basin (Andrews et al., 1985) and in the extensional Eastern Morongo basin in California (Kulongoski et al., 2005).

The variability in the magnitude of helium degassing fluxes in the Amos region could indicate localized sources of helium emplaced at lower depths, as observed in other continental settings (e.g., Kulongoski et al., 2005) as well as different recharge levels in different areas. The helium source could be local Archean and Proterozoic magmatic plutons such as the monozogranitic intrusion of La Motte (Fig. 1a), which contain up to 18 ppm U and 9.5 ppm of Th in localized quartz veins (Mulja et al., 1995). Terrigenic helium could be driven toward the surface by tectonic accidents (faults) such as those affecting the southern part of the SMB esker (TSSM-P1, -P3 and -P5 well nest).

Estimated $^4\text{He}_{terr}$ fluxes can be cross validated by calculating U–Th/^4He ages of groundwater in SMB and Harricana eskers, and to obtain independent water ages for the wells in the clay plain. The U–Th/^4He age "t" is calculated using equation (e.g., Torgersen and Clarke, 1985; Kulongoski et al., 2003):

$$t = \frac{[^4\text{He}_{terr}]}{P_{4\text{He}} \cdot \Lambda_{4\text{He}} \cdot \left(\frac{1-\phi}{\phi}\right) \cdot \rho_{rock} + \frac{J_0}{z_x \phi \rho_{water}}} \qquad (10)$$

The density of rock (ρ_{rock}) and water (ρ_{water}) are assumed to be 2.65 and 1 g cm^{-3}, respectively. z_x is the depth (m) at which this flux enters the aquifer, taken as the distance from the mid-screen in the well casing to the contact with the basement (Kulogonski et al., 2005). For the unscreened bedrock wells Landrienne, 101CH and 55HB we used the total thickness of the bedrock aquifer, i.e., 89.6 m (Landrienne), 10.67 m (101CH) and 97.30 m

(55HB), respectively (Table 2). Porosities of 25–30% and calculated helium fluxes (Fig. 6a–f) were used in these calculations. For the basal fractured aquifer, Cloutier et al. (2013) assume porosities of less than 10% (here taken as a maximum value). The $P_{4\text{He}}$ production rate is assumed to range between $1.33 \pm 0.64 \times 10^{-13}$ $\text{cm}^3\text{STP g}_{rock} \text{yr}^{-1}$ (this study) and the local crustal value of 6.40×10^{-13} $\text{cm}^3\text{STP g}_{rock} \text{yr}^{-1}$ (Pinti et al., 2011).

The apparent $^4\text{He}_{terr}$ gradients in Fig. 5a suggests that clay plain wells Landrienne and 55HB are affected by the same helium flux than that entering the bottom of the Harricana esker (2.0–2.7×10^{-8} $\text{cm}^3\text{STP cm}^{-2} \text{yr}^{-1}$) but different levels of freshwater input as seen in many other aquifers with Harricana having the highest freshwater dilution levels (e.g., Castro et al., 2000, 2005; Patriarche et al., 2004). On the other hand, modeling results suggest that Barraute and 101CH, which are part of a different system, have a helium flux comparable to those estimated in the SMB esker (8.0–8.5×10^{-8} $\text{cm}^3\text{STP cm}^{-2} \text{yr}^{-1}$ to 5.8–6.6×10^{-7} $\text{cm}^3\text{STP cm}^{-2} \text{yr}^{-1}$).

Calculated U–Th/^4He ages are reported in Table 2 and Fig. 1b. Uncertainties have been calculated as propagated errors including those for helium fluxes, *in situ* production rates and porosity (Table 2). However, model age errors can be considerably higher, over 50% (Torgersen and Clarke, 1985) depending on natural parameter variations, including porosity, rock density, U and Th concentration distribution and helium fluxes, which are a first order approximation due to the simplifications implemented in the model (Ma et al., 2005).

Calculated U–Th/^4He groundwater ages for the SMB esker range from 3.0 ± 0.1 a (TSSM-P1) to 272 ± 9 a (TSAM-P2). Most wells display U–Th/^4He ages within the same order of magnitude of those estimated by $^3\text{H}/^3\text{He}$.

Calculated U–Th/^4He ages for the Harricana wells are higher (41.0 ± 1.9–121.2 ± 9.4 a) than the calculated $^3\text{H}/^3\text{He}$ ages (6.6 ± 1.1–9.9 ± 0.9 a; Table 2). It is very common to obtain ages that do not agree using different methods (see e.g., Castro and Goblet, 2005). Assuming fluxes of 0.8–6.6×10^{-7} $\text{cm}^3\text{STP cm}^{-2} \text{yr}^{-1}$, equal to those estimated for the SMB esker, we obtain ages similar to those calculated using the $^3\text{H}/^3\text{He}$ method.

The U–Th/^4He method can be useful to determining groundwater residence times of the buried Barraute esker and those in the fractured bedrock under the plain (Landrienne, 55HB and 101CH) for which tritium data is not available. Groundwater from the fractured basement displays ages varying between 1473 ± 292 a for the Landrienne municipality well to 137 ± 28 ka for the most saline and deep groundwater form well 55H. Domestic well CH101 groundwater has U–Th/^4He ages from 28 ± 1 a to 208 ± 6 a; Barraute groundwater exhibits U–Th/^4He ages between 8.7 ± 0.2 and 65 ± 3 a (Table 2). The wide range of calculated U–Th/^4He water ages for these two last wells is depending on the chosen helium flux which is highly variable in the area (8.0×10^{-8}–6.6×10^{-7} $\text{cm}^3\text{STP cm}^{-2} \text{yr}^{-1}$; Fig. 6). These variable fluxes can also account for the mismatch between $^3\text{H}/^3\text{He}$ ages and U–Th/^4He ages for the younger waters (Table 2).

The Barraute esker is buried and does not receive direct recharge. Veillette et al. (2007) suggested that the Barraute recharge might originate from water infiltrated through the Harricana moraine, in particular from the elevated area of Mont Video (Fig. 1), 10 km west of the Barraute esker. The piezometric map produced by Cloutier et al. (2013) shows a major hydraulic gradient (0.014 m/m) between Mont Video and Barraute esker. Assuming a travel time between these two structures of 9–65 a, horizontal flow velocities of 3.5–4.9×10^{-6} ms^{-1} can be derived. For porosities ranging between 10% (if the flow is through glacial tills and fractured bedrock) and 25–30% (if flow is through buried granular aquifers), the calculated average horizontal hydraulic conductivities K_x range between 3.48×10^{-5} and 7.5×10^{-4} ms.
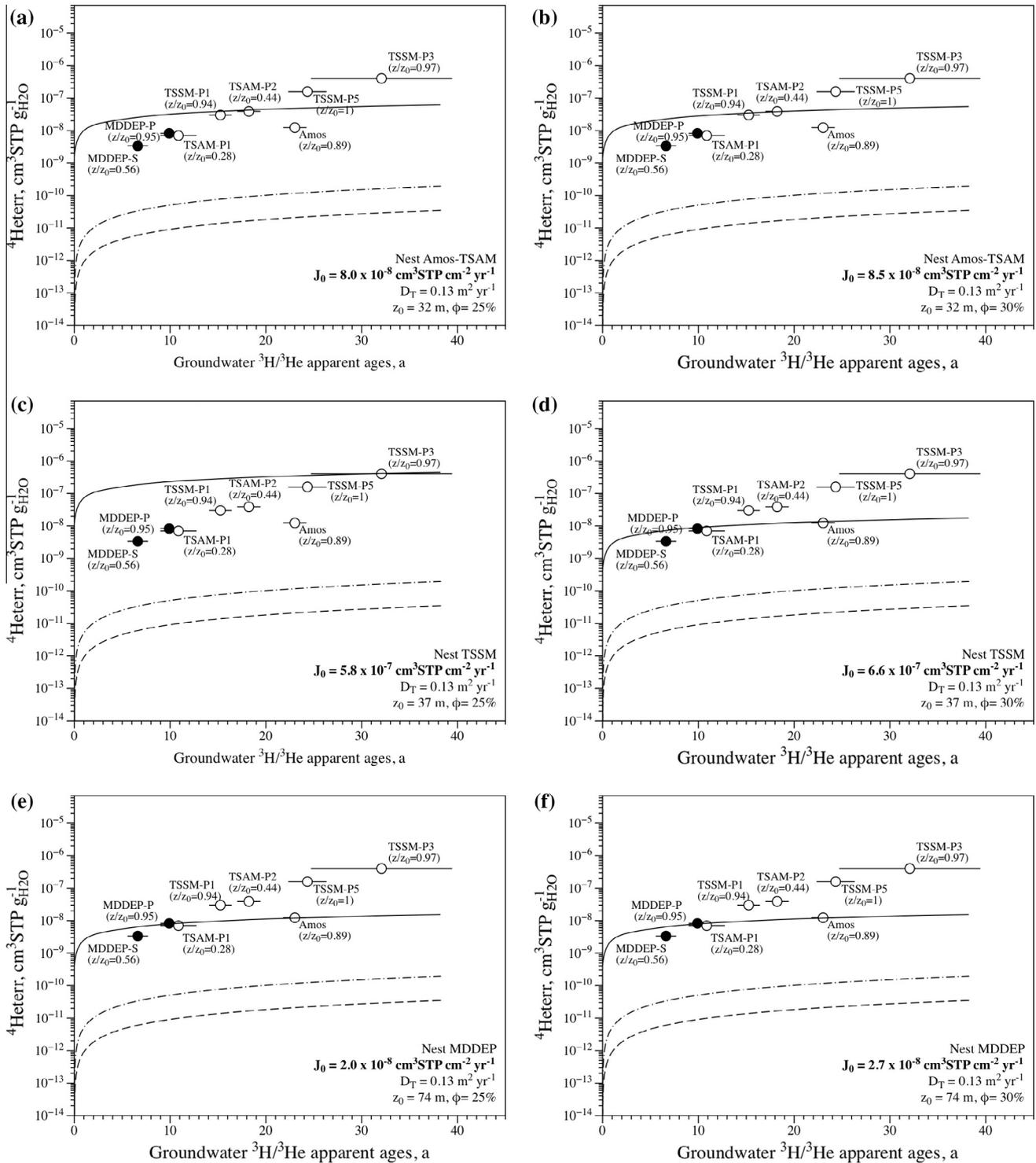
Fig. 6. Evolution of the $^4He_{terr}$ concentrations in groundwater plotted as a function of the calculated $^3H/^3He$ apparent ages. Plain curves (a–f) represent the simulated evolution of the $^4He_{terr}$ concentration in groundwater as a function of age for the three well nest geographically identified in the study area, i.e., Amos, TSAM-P1 and -P2 (a–b); TSSM-P1 and -P2, (TSSM-P5) (c–d); MDEEP-S and MDDEP-P (e–f), and for aquifer porosities of 25–30%. Dashed and dash and dot curves represent the simulated evolution of the $^4He_{terr}$ concentration in groundwater as a function of age based exclusively on *in situ* production using P_{4He} rate of 1.33×10^{-13} and 6.40×10^{-13} cm³STP g rock yr⁻¹, respectively.

Cloutier et al. (2013) calculated hydraulic conductivities K_x for till deposits, fractured bedrock and esker/moraine of 9.3×10^{-7}–1.4×10^{-4} ms⁻¹, 5.0×10^{-9}–4.3×10^{-5} ms⁻¹ and 4.9×10^{-6}–3.2×10^{-1} ms⁻¹, respectively. Hydraulic conductivities calculated for the aquifer between Barraute and Mont Video are in the upper end of the estimates by Cloutier et al. (2013) suggesting

that there is a continuum between the granular structure of the Harricana moraine and that of the Barraute esker, allowing for fast recharge.

U–Th/^{4}He age estimations suggest that older waters reside in the fractured bedrock below the glaciofluvial formations. Maximum U–Th/^{4}He ages in the fractured bedrock aquifer range

from 1472 ± 292 a for groundwater tapped by the Landrienne municipality well up to 137 ± 28 ka for the most saline and deepest groundwater found in domestic well 55HB (Fig. 1b). These ages suggest that the Superior Province bedrock aquifer could have preserved isolated pockets of fossil meltwater following the penultimate (Illinoian, marine isotope stage, MIS, 6) and last glaciations (Wisconsinan, MIS 2) (Lisiecki and Raymo, 2005). This postglacial water, which accumulated large amounts of radiogenic ^{4}He may have mixed with younger, post-bomb water enriched in tritiogenic ^{3}He, flowing rapidly in the aquifers closer to the top of the esker structures.

6. Conclusions

Noble gas isotopic compositions of groundwater circulating in eskers (SMB and Barraute) and interlobate glaciofluvial sediments (Harricana moraine) of the Amos region in northwester Quebec show the presence of anthropogenic, terrigenic and atmospheric helium. These helium components reflect the occurrence of large-scale mixing between different water bodies having evolved in different geological environments. The esker aquifers contain at least two types of groundwater. The first one flows through the highly porous and permeable sandy and gravely layers forming these glaciofluvial landforms. It contains variable amounts of post-bomb tritiogenic ^{3}He and ^{3}H/^{3}He ages point to modern water, recharged recently (<32 years). The second type of groundwater may be considered fossil, likely consisting of glacial meltwater trapped within the fractured volcano-metamorphic bedrock aquifer that underlie the eskers and moraines. These fossil waters mix with the younger waters at the top of the eskers, releasing considerable amounts of radiogenic ^{4}He. Exchange between these two groundwater masses are clearly evidenced by (helium) concentrations, isotopic and salinity gradients (Fig. 5a–d), and have been modeled here as helium fluxes entering the base of the esker and moraine aquifers (Fig. 6a–f).

These results further document the stratification of the water in the aquifers present in these deglacial landforms, as suggested by Riverin (2006), whereby old water ($\geqslant$6000 a based on uncorrected ^{14}C ages and $\geqslant$1000 a based on U–Th/^{4}He ages; this study) may be found in the confined (basal) part of the eskers and modern water in the unconfined (upper) part of the eskers, close to the top of the structure. Noble gases were also used to constrain the water ages present and the occurrence of possible mixing between the different water masses.

Calculated groundwater ages have important implications for the sustainable management of this precious freshwater resource. This resource needs to be preserved from overexploitation since the deeper portion of these aquifers is not renewed on a human timescale ($\geqslant$1000 a old). Furthermore, short water residence times clearly indicate that the resource is at risk of being contaminated in addition to being subjected to climatic stresses. It is worth noting that in this region, eskers are the sites of numerous activities, such as sand and gravel extraction and old urban and sanitary waste repositories. If these sites are not properly managed, pollution from chemicals through highly permeable aquifers where flow is rapid could seriously compromise the groundwater resource.

Acknowledgements

References

Aeschbach-Hertig, W., Schlosser, P., Stute, M., Simpson, H.J., Ludin, A., Clark, J.F., 1998. A ^{3}H/^{3}He study of groundwater flow in a fractured bedrock aquifer. Ground Water 36, 661–670.

Aeschbach-Hertig, W., Beyerle, U., Holocher, J., Peeters, F., Kipfer, R., 2001. Excess air in groundwater as a potential indicator of past environmental changes. In: International Conference on the Study of Environmental Change Using Isotope Techniques IAEA-CN-80/29. IAEA, Wien, pp. 34–36.

Andrews, J.N., Lee, P.J., 1979. Inert gases in groundwater from the Bunter Sandstone of England as indicators of age and paleoclimatic trends. J. Hydrol. 41, 233–252.

Andrews, J.N., Goldbrunner, J.E., Darling, W.G., Hooker, P.J., Wilson, G.B., Youngman, M.J., Eichinger, L., Rauert, W., Stichler, W., 1985. A radiochemical, hydrochemical and dissolved gas study of groundwaters in the Molasse basin of Upper Austria. Earth Planet. Sci. Lett. 73, 317–332.

Ballentine, C.J., Burnard, P.G., 2002. Production, release and transport of noble gases in the continental crust. Rev. Mineral. Geochem. 47, 481–538.

Ballentine, C.J., Hall, C.M., 1999. Determining paleotemperature and other variables by using an error-weighted, nonlinear inversion of noble gas concentrations in water. Geochim. Cosmochim. Acta 63, 2315–2336.

Banerjee, I., McDonald, B.C., 1975. Nature of esker sedimentation. In: Jopling, A.V., Mc-Donald, B.C. (Eds.), Glaciofluvial and glaciolacustrine sedimentation. Soc. Econom. Paleontol. Mineral. Spec. Publ. vol. 23, pp. 132–154.

Benson, B.B., Krause, D., 1980. Isotopic fractionation of helium during solution: A probe for the liquid state. J. Solut. Chem. 9, 895–909.

Boulton, G.S., Caban, P.E., Van Gijssel, K., 1995. Groundwater flow beneath ice sheets: Part I – Large scale patterns. Quat. Sci. Rev. 14, 545–562.

Boulton, G.S., Hagdorn, M., Maillot, P.B., Zatsepin, S., 2009. Drainage beneath ice sheets: groundwater–channel coupling, and the origin of esker systems from former ice sheets. Quat. Sci. Rev. 28, 621–638.

Castelli, S. 2012. Hydrogéochimie des sources associées aux eskers de l'Abitibi, Québec. MSc Thesis. Montréal, Département de génies civil, géologique et des mines, École Polytechnique de Montréal, 107 p.

Castelli, S., Cloutier, V., Blanchette, D., 2011. Hydrogéochimie et qualité de l'eau des sources associées aux eskers de l'Abitibi, Québec. Proceedings, Geohydro 2011, Joint/IAH-CNC, Québec, 4 p.

Castro, M.C., Goblet, P., 2005. Calculation of groundwater ages – a comparative analysis. Ground Water 43, 368–380.

Castro, M.C., Goblet, P., Ledoux, E., Violette, S., de Marsily, G., 1998. Noble gases as natural tracers of water circulation in the Paris Basin 2. Calibration of a groundwater flow model using noble gas isotope data. Water Resour. Res. 34, 2467–2483.

Castro, M.C., Stute, M., Schlosser, P., 2000. Comparison of ^{4}He ages and ^{14}C ages in simple aquifer systems: implications for groundwater flow and chronologies. Appl. Geochem. 15, 1137–1167.

Castro, M.C., Patriarche, D., Goblet, P., 2005. 2-D numerical simulations of groundwater flow, heat transfer and ^{4}He transport – implications for the He terrestrial budget and the mantle helium-heat imbalance. Earth Planet. Sci. Lett. 237, 893–910.

Clark, I.D., Fritz, P., 1997. Environmental Isotopes in Hydrogeology. CRC Press, 352 p.

Clark, P.U., Walder, J.S., 1994. Subglacial drainage, eskers, and deforming beds beneath the Laurentide and Eurasian ice sheets. GSA Bull. 106, 304–314.

Cloutier, V., Veillette, J., Roy, M., Gagnon, F., Bois, D., 2007. Regional hydrogeochemistry of groundwater in fractured Canadian Shield rock and glaciofluvial formations in Abitibi, Québec. In: Proceedings, 60th Canadian Geotechnical Conference and 8th Joint CGS/IAH-CNC Groundwater Conference, Ottawa, pp. 355–362.

Cloutier, V., Aubert, T., Audet-Gagnon, F., Blanchette, D., Castelli, S., Cheng, L. Z., Dallaire, P.-L., Fallara, F., Godbout, G., Nadeau, S., Pitre, O., Rey, N., Roy, M., Veillette, J.J., 2011. Projet d'acquisition de connaissances sur les eaux souterraines de l'Abitibi-Témiscamingue, Québec. In: Proceedings, Geohydro 2011, Joint/IAH-CNC, Québec, 4 p.

Cloutier, V., Blanchette, D., Dallaire, P.-L., Nadeau, S., Rosa, E., Roy, M. 2013. Projet d'acquisition de connaissances sur les eaux souterraines de l'Abitibi-Témiscamingue (partie 1). Research report P001. GRES, IRME, Université du Québec en Abitibi-Témiscamingue, 135 p.

Dyke, A.S., 2004. An outline of North American deglaciation with emphasis on central and northern Canada. In: Ehlers, J., Gibbard, P.L. (Eds.), Quaternary Glaciations – Extent and Chronology, Part II: North America. Elsevier, Amsterdam, pp. 373–424.

Freeze, R.A., Cherry, J.A., 1979. Groundwater. Prentice-Hall Inc., Englewood Cliffs, New Jersey.

Heaton, T.H.E., Vogel, J.C., 1981. "Excess air" in groundwater. J. Hydrol. 50, 201–216.

Heemskerk, A.R., Johnson, J., 1998. Tritium Analysis: Technical Procedure 1.0. University of Waterloo, Waterloo, ON.

IAEA/WMO (International Atomic Energy Agency/World Meteorological Organization). 2004b. Global network of isotopes in precipitation. The GNIP database. Available at: <http://isohis.iaea.org>.

Kinzelbach, W., et al., 2002. A survey of methods for analysing groundwater recharge in arid and semi-arid regions, Division of Early Warning and Assessment. United Nations Environmental Program. UNEP/DEWA/RS.02-2.

Kulongoski, J.T., Hilton, D.R., Izbicki, J.A., 2003. Helium isotope studies in the Mojave Desert, California: implications for groundwater chronology and regional seismicity. Chem. Geol. 202, 95–113.

Kulongoski, J.T., Hilton, D.R., Izbicki, J.A., 2005. Source and movement of helium in the eastern Morongo groundwater Basin: the influence of regional tectonics on crustal and mantle helium fluxes. Geochim. Cosmochim. Acta 69, 3857–3872.

Lisiecki, L., Raymo, M.R., 2005. A Pliocene-Pleistocene stack of 57 globally distributed benthic d18O records. Paleocean. vol 20, No. 1, PA100310 (1029/2004PA001071).

Lucas, L.L., Unterweger, M.P., 2000. Comprehensive review and critical evaluation of the half-life of tritium. J. Res. Natl. Inst. Stand. Technol. 105, 541–549.

Lupton, J.E., 1983. Terrestrial inert gases: isotope tracer studies and clues to primordial components in the mantle. Annu. Rev. Earth Planet. Sci. 11, 371–414.

Ma, L., Castro, M.C., Hall, C.M., Walter, L.M., 2005. Cross-formational flow and salinity sources inferred from a combined study of helium concentrations, isotopic ratios and major elements in the Marshall aquifer, southern Michigan. Geochem. Geophys. Geosyst. 6 (10), Q10004. http://dx.doi.org/10.1029/2005GC001010.

Marty, B., 1984. On the noble gas isotopic fractionation in naturally occurring gases. Geochem. J. 18, 157–162.

Marty, B., Torgersen, T., Meynier, V., O'Nions, R.K., de Marsily, G., 1993. Helium isotope fluxes and groundwater ages in the Dogger Aquifer, Paris Basin. Water Resour. Res. 29, 1025–1035.

Matsuda, J., Matsumoto, T., Sumino, H., Nagao, K., Yamamoto, J., Miura, Y., Kaneoka, I., Takahata, N., Sano, Y., 2002. The ^{3}He/^{4}He ratio of the new internal He standard of Japan (HESJ). Geochem. J. 36, 191–195.

Morrison, P., Pine, J., 1955. Radiogenic origin of the helium isotopes in rocks. Ann. N.Y. Acad. Sci. 62, 69–92.

Mulja, T., Williams-Jones, A., Wood, S., Boily, M., 1995. Geology and mineralogy: the rare-element-enriched monzogranite-pegmatite-quartz vein systems in the Preissac-La Corne batholith, Quebec. Can. Mineral. 33, 793–815.

Nadeau, S. 2011. Estimation de la ressource granulaire et du potentiel aquifère des eskers de l'Abitibi-Témiscamingue et du sud de la Baie-James (Québec). Msc Thesis, Université du Québec à Montréal (UQÀM), Montreal, 145 p.

O'Nions, R.K., Oxburgh, E.R., 1983. Heat and helium in the earth. Nature 306, 429–431.

Ozima, M., Podosek, F.A., 1983. Noble Gas Geochemistry. Cambridge University Press, Cambridge.

Patriarche, D., Castro, M.C., Goblet, P., 2004. Large-scale hydraulic conductivities inferred from three-dimensional groundwater flow and ^{4}He transport modeling in the Carrizo aquifer, Texas. J. Geophys. Res. 109, B11202. http://dx.doi.org/10.1029/2004JB003173.

Pinti, D.L., Béland-Otis, C., Tremblay, A., Castro, M.C., Hall, C.M., Marcil, J.-S., Lavoie, J.-Y., Lapointe, R., 2011. Fossil brines preserved in the St-Lawrence Lowlands, Québec, Canada as revealed by their chemistry and noble gas isotopes. Geochim. Cosmochim. Acta 75, 4228–4243.

Riverin, M.N. 2006. Caractérisation et modélisation de la dynamique d'écoulement dans le système aquifère de l'esker Saint-Mathieu–Berry, Abitibi, Québec. Msc Thesis, INRS-ETE, Quebec, 181 p.

Roy, M., Dell'Oste, F., Parent, M., Veillette, J.J., de Vernal, A., Hélie, J.-F., Parent, M., 2011. Insights on the events surrounding the final drainage of Lake Ojibway based on James Bay stratigraphic sequences. Quat. Sci. Rev. 30, 682–692.

Sano, Y., Takahata, N., Igarashi, G., Koizumi, N., Sturchio, N.C., 1998. Helium degassing related to the Kobe earthquake. Chem. Geol. 150, 171–179.

Sano, Y., Tokutake, T., Takahata, N., 2008. Accurate measurement of atmospheric helium isotopes. Anal. Sci. 24, 521–525.

Sano, Y., Marty, B., Burnard, P., 2013. Noble gases in the atmosphere. In: Burnard, P. (Ed.), The Noble Gases as Geochemical Tracers, Advances in Isotope Geochemistry. Springer-Verlag, Berlin Heidelberg, pp. 17–31.

Schlosser, P., Stute, M., Sonntag, C., Munnich, K.O., 1989. Tritiogenic ^{3}He in shallow groundwaters. Earth Planet. Sci. Lett. 94, 245–256.

Shilts, W.W., Aylsworth, J.M., Kaszycki, C.A., Klassen, R.A., 1987. In: Graf, W.L. (Ed.), Canadian Shield: Geomorphic systems of North America. Boulder, Colorado, Geological Society of America, Centennial Special 2, pp. 119–150.

Smith, S.P., Kennedy, B.M., 1983. The solubility of noble gases in water and NaCl brine. Geochim. Cosmochim. Acta 47, 503–515.

Solomon, D.K., Schiff, S.L., Poreda, R.J., Clarke, W.B., 1993. A validation of the ^{3}H/^{3}He method for determining groundwater recharge. Water Resour. Res. 29 (2951–2962), 1993.

Solomon, D.K., Hunt, A., Poreda, R.J., 1996. Source of radiogenic helium 4 in shallow aquifers: implications for dating young groundwater. Water Resour. Res. 32, 1805–1813.

Stute, M., Schlosser, P., 1993. Principles and applications of the noble gas paleothermometer. In: Swart, P.K., Lohmann, K.C., McKenzie, J., Savin, S. (Eds.), Climate Change in Continental Isotopic Records. AGU, Washington DC, pp. 89–100.

Stute, M., Sonntag, C., Déak, J., Schlosser, P., 1992. Helium in deep circulating groundwater in the Great Hungarian Plain: flow dynamics and crustal and mantle helium fluxes. Geochim. Cosmochim. Acta 56, 2051–2067.

Takaoka, N., Mizutani, Y., 1987. Tritiogenic ^{3}He in groundwater in Takaoka. Earth Planet. Sci. Lett. 85, 74–78.

Tolstikhin, I.N., Kamenskiy, I.L., 1969. Determination of ground-water ages by T–He-3 method. Geochem. Int. 6, 810–811.

Torgersen, T., 2010. Continental degassing flux of ^{4}He and its variability. Geochem. Geophys. Geosyst. 11, Q06002. http://dx.doi.org/10.01029/02009GC002930.

Torgersen, T., Clarke, W.B., 1985. Helium accumulation in groundwater, I: an evaluation of sources and the continental flux of crustal ^{4}He in the Great Artesian Basin, Australia. Geochim. Cosmochim. Acta 49, 1211–1218.

Torgersen, T., Ivey, G.N., 1985. Helium accumulation in groundwater, II: Mechanisms for the accumulation of the crustal ^{4}He degassing flux. Geochim. Cosmochim. Acta 49, 2445–2452.

Veillette, J.J., 1994. Evolution and paleohydrology of glacial lakes Barlow and Ojibway. Quat. Sci. Rev. 13, 945–971.

Veillette, J.J., 1996. Géomorphologie et géologie du Quaternaire du Témiscamingue, Québec et Ontario. Geol. Surv. Canada Bull. 476, 6 maps 1/100,000, Ottawa, 269 p.

Veillette, J.J., Paradis, S.J., Thibaudeau, P., 2003. Les cartes de formation en surface de l'Abitibi. Geological Survey of Canada, Open File 1523, 10 maps, 1:100,000 scale.

Veillette, J.J., Maqsoud, A., De Corta, H., Bois, D., 2004. Hydrogéologie des eskers de la MRC d'Abitibi, Québec. In: 57th Canadian Geotechnical Conference, 5th Joint CGS/IAH-CNC Conference, Québec city, October 2004, Session 3B2, pp. 6–13.

Veillette, J.J., Cloutier, V., de Corta, H., Gagnon, F., Roy, M., Douma, M., Bois D., 2007. A complex recharge network, the Barraute Esker, Abitibi, Québec. In: Proceedings, 60th Canadian Geotechnical Conference and 8th Joint CGS/IAH-CNC Groundwater Conference, Ottawa, pp. 347–354.

Vogel, J.C., 1967. Investigation of groundwater flow with radiocarbon. In Isotopes in Hydrology, 355–369. IAEA-SM 83/24, Vienna, Austria, pp. 355–368.

Weber, W.W., Latulippe M., 1964. Amos-Barraute Area, Abitibi East County: Quebec Dept. Nat. Resour. Mines Branch Geol. Report G. R., 109 p.

Weise, S., Moser, H., 1987. Groundwater Dating with Helium Isotopes. Techniques in Water Resource Development. IAEA, Wien, pp. 105–126.